Ferromagnetic $Mn_5Ge_3C_{0.8}$ contacts on Ge: work function and specific contact resistivity

2013 Semicond. Sci. Technol. 28 125002

(http://iopscience.iop.org/0268-1242/28/12/125002)

Semicond. Sci. Technol. **28** (2013) 125002 (5pp) doi:10.1088/0268-1242/28/12/125002

Ferromagnetic $Mn_5Ge_3C_{0.8}$ contacts on Ge: work function and specific contact resistivity

I A Fischer[1], J Gebauer[1], E Rolseth[1], P Winkel[2], L-T Chang[3], K L Wang[3], C Sürgers[2] and J Schulze[1]

[1] Institut für Halbleitertechnik (IHT), Universität Stuttgart, Pfaffenwaldring 47, Stuttgart, D-70569, Germany
[2] Physikalisches Institut, Karlsruhe Institute of Technology, Wolfgang-Gaede-Str. 1, Karlsruhe, D-76131, Germany
[3] Device Research Laboratory, Department of Electrical Engineering, University of California, Los Angeles, CA 90095, USA

E-mail: fischer@iht.uni-stuttgart.de

Received 24 June 2013, in final form 9 September 2013
Published 24 October 2013
Online at stacks.iop.org/SST/28/125002

Abstract
We report on the study of the electrical and magnetic properties of $Mn_5Ge_3C_{0.8}$ contacts deposited on highly doped n-Ge (1 0 0) as a potentially complementary metal–oxide–semiconductor (CMOS)-compatible material system for spin injection into Ge. $Mn_5Ge_3C_{0.8}$ is a ferromagnet with a Curie temperature of 445 K and with a resistivity that is comparable to highly doped Ge. We extract the work function of $Mn_5Ge_3C_{0.8}$ from metal–oxide–semiconductor capacitance measurements and obtain a specific contact resistivity $r_C = 5.0\ \Omega\ cm^2$ from transmission-line measurements. We discuss possible origins of the large specific contact resistivity of $Mn_5Ge_3C_{0.8}$ on Ge.

(Some figures may appear in colour only in the online journal)

1. Introduction

Electronic devices based on spin transport and realized in materials compatible with complementary metal–oxide–semiconductor (CMOS) technology are currently being investigated as possible alternatives to CMOS transistor logic. A necessary prerequisite for many device proposals that make use of the electron spin is the efficient injection of spin-polarized electrons into the semiconductor body of the device [1, 2], which can be achieved by using ferromagnetic metal contacts. However, spin injection from a direct metal–semiconductor contact typically suffers from the conductivity mismatch problem [3]: in the diffusive regime, the fraction of spin polarized electrons injected into the semiconductor is proportional to $\sigma_{SC}/\sigma_F \ll 1$, where σ_{SC} (σ_F) is the conductivity of the semiconductor (ferromagnet). This problem can be circumvented, e.g., by inserting a tunnel contact at the interface between semiconductor and ferromagnet [4]. Injection of spin-polarized electrons into Si [5–7] and, more recently, Ge [8–10] has been achieved from tunnel contacts or Schottky contacts. For future device applications, source and drain contacts with low contact resistances would be desirable.

Alternatively, a ferromagnetic 'bad metal' with a high resistivity may be used. If the resistivities of the ferromagnetic contact and the doped semiconductor are comparable, spin injection from a low-resistive ohmic contact between the semiconductor and the ferromagnet becomes possible in principle. In this work, we investigate $Mn_5Ge_3C_{0.8}$ as a candidate for spin injection into Ge. The Ge-based parent compound Mn_5Ge_3 is a ferromagnet with a Curie temperature $T_C = 296$ K. Its spin polarization measured by Andreev reflection has been found to be (42 ± 5)% [11] and a value of (15 ± 5)% has been obtained by spin-resolved photoelectron spectroscopy measurements [12]. Mn_5Ge_3 grows epitaxially on Ge (1 1 1) with a sheet resistance comparable to highly doped ($N_D > 10^{20}\ cm^{-3}$) Ge [13, 14]. The high Curie temperature and the atomically sharp interface to Ge (1 1 1) have already motivated investigations of

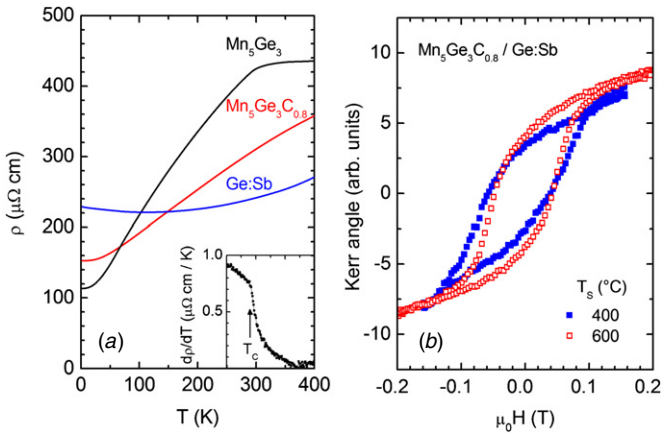

Figure 1. (*a*) Resistivity of 50 nm thick Mn_5Ge_3 and $Mn_5Ge_3C_{0.8}$ layers deposited on insulating (11$\bar{2}$0)-oriented sapphire substrates at $T_S = 400$ °C and 500 °C, respectively, and of 40 nm thick n-Ge (1 0 0) with $N_D = 1 \times 10^{20}$ cm^{-3}. Inset shows the derivative $d\rho/dT$ of the Mn_5Ge_3 film indicating a Curie temperature $T_C \approx 296$ K. (*b*) Magnetic hysteresis loops obtained from magneto-optic Kerr effect measurements on $Mn_5Ge_3C_{0.8}$ deposited at different T_S on n-Ge (1 0 0) with $N_D = 1 \times 10^{20}$ cm^{-3} showing no degradation of hysteresis.

Mn_5Ge_3/Ge (1 1 1) Schottky contacts for spin injection [15]. The Curie temperature of Mn_5Ge_3 can be enhanced by C-doping [16–18] and has been shown to attain 445 K, which is considerably above room temperature. This makes C-doped Mn_5Ge_3 even more interesting as a candidate for spin injection. Here, we characterize $Mn_5Ge_3C_{0.8}$ contacts deposited by magnetron sputtering on highly doped n-Ge (1 0 0). This is motivated by the fact that this crystal plane orientation is most common in CMOS technology. We determine the work function of $Mn_5Ge_3C_{0.8}$ from metal–oxide–semiconductor (MOS) capacitances and find that the $Mn_5Ge_3C_{0.8}$/Ge (1 0 0) contacts show ohmic behavior but exhibit high specific contact resistivities.

2. Experimental details

As a first step, we investigated the resistivity of the $Mn_5Ge_3C_{0.8}$ layers and their magnetic properties. $Mn_5Ge_3C_{0.8}$ layers with a thickness of 50 nm were deposited on insulating sapphire at substrate temperatures T_S = 400–500 °C by simultaneous dc- and rf-magnetron sputtering from elemental targets of Mn, Ge and C in a high-vacuum system under Ar atmosphere [16, 17]. The temperature dependences of the resistivity ρ for Mn_5Ge_3 and $Mn_5Ge_3C_{0.8}$ measured by a four-point probe are shown in figure 1 (*a*) and compared to the temperature-dependent resistivity of Sb-doped Ge ($N_D = 1 \times 10^{20}$ cm^{-3}) also shown in figure 1 (*a*). While $\rho(T)$ of Mn_5Ge_3 shows a clear kink at the Curie temperature $T_C = 296$ K, no signature of a magnetic phase transition is observed in $\rho(T)$ of $Mn_5Ge_3C_{0.8}$ indicating $T_C > 400$ K. The resistivity $\rho_{MnGeC} = 300$ $\mu\Omega$ cm at 300 K agrees well with ρ of degenerately doped ($N_D > 10^{20}$ cm^{-3}) Ge. The highest T_C values have been obtained for $Mn_5Ge_3C_x$ films sputtered at $T_S = 410$ °C on sapphire [16]. Moreover, epitaxially grown $Mn_5Ge_3C_{0.6}$ films on Ge (1 1 1) remain ferromagnetic after annealing at 750 °C albeit with a reduced $T_C = 350$ K [19]. Therefore, in this work, $Mn_5Ge_3C_{0.8}$ films were deposited on n-Ge (1 0 0) with $N_D = 1 \times 10^{20}$ cm^{-3} for different substrate temperatures in the range 400 °C < T_S <600 °C. Figure 1 (*b*) shows magnetic hysteresis loops measured by the magneto-optic Kerr effect at room temperature. The variation of T_S between 600 °C and 400 °C does not considerably change the magnetization curve. Hence, it is possible to integrate the fabrication of $Mn_5Ge_3C_{0.8}$ contacts into a low thermal budget process for Ge device fabrication.

For the investigation of the work function of $Mn_5Ge_3C_{0.8}$ and its contact properties on n-Ge, we fabricated MOS capacitors, transmission-line measurement (TLM) structures and Schottky diodes. The fabrication of MOS capacitors started by deposition of 80 nm PECVD oxide on a p$^-$-Si (1 0 0) substrate (ρ > 3–5 Ω cm and $N_A \approx 10^{15}$ cm^{-3}). Subsequently, 40 nm of $Mn_5Ge_3C_{0.8}$ was deposited at a substrate temperature $T_S = 450$ °C. The sample was capped with 40 nm of Al without breaking the vacuum in order to protect the $Mn_5Ge_3C_{0.8}$ from oxidation. Another 300 nm of Al was deposited *ex situ* by thermal evaporation as the top metallization layer. Finally, the Al and $Mn_5Ge_3C_{0.8}$ metal contacts were defined by standard photolithography and structured in one etching step to obtain circular MOS capacitances.

For the TLM and Schottky-diode structures, device fabrication started with deposition of a virtual Ge substrate with a thickness of 50 nm on a p$^-$-Si (1 0 0) substrate (ρ > 3–5 Ω cm) by molecular beam epitaxy (MBE). The virtual substrate serves to accommodate the difference in lattice constant between the Si substrate and final Ge layer and enables the subsequent growth of high-quality Ge layers. On the virtual substrate, a Sb-doped n-Ge layer ($N_D = 1 \times 10^{20}$ cm^{-3}) with a thickness of 40 nm was grown. After structuring the mesa by reactive ion etching (RIE), an oxide layer (150 nm) was deposited by PECVD to protect the surface. After removal of the oxide by wet etching with HF, 40 nm of $Mn_5Ge_3C_{0.8}$ was deposited by sputtering at a substrate temperature T_S = 450 °C (500 °C) for sample A(B) and subsequently capped with 40 nm of Al without breaking the vacuum. Another 400 nm of Al was then deposited by evaporation as the final metallization layer. The Al- and $Mn_5Ge_3C_{0.8}$-metallization was structured in one etching step. The schematics of all fabricated devices are shown in the inset of figure 2 as well as in figures 3(*a*) and 5(*a*).

3. Results and discussion

The *C*–*V* characteristics of the MOS capacitors are shown in figure 2. From the average capacitance $C_{OX} = 2.66 \times 10^{-10}$ F, obtained from measurements of two circular capacitors with radius r = 451 μm each, the average flat-band voltage $V_{FB} = -2.573$ V and the oxide charges $Q_{eff} = (6.523 \pm 0.243) \times 10^{11}$ cm^{-2}, we extract a work function difference $\Phi_{MS} = -(0.063 \pm 0.094)$ eV. Here, V_{FB} was obtained from the *C*–*V* characteristics with the flatband capacitance method [20] and Q_{eff} was obtained from reference MOS capacitors fabricated without the $Mn_5Ge_3C_{0.8}$ layer. Using [21]

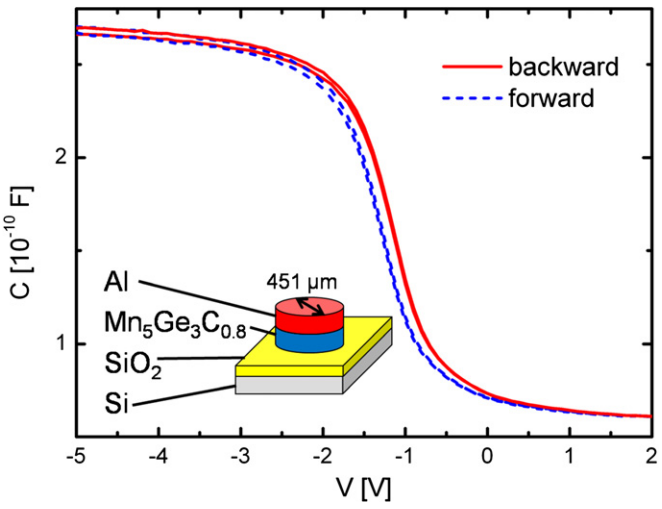

Figure 2. *C–V* characteristics obtained from two circular MOS capacitors with radius $r = 451$ μm as shown in the inset. Both the forward (from negative to positive voltages) and the backward (from positive to negative voltages) sweep are shown for each sample. We obtain $\Phi_M = 4.237$ V as the work function of $Mn_5Ge_3C_{0.8}$ from the measurements.

$$\Phi_M = \Phi_{MS} + \left(\chi_{Si} + \frac{E_g}{2} - k_B T \ln\left(\frac{N_A}{n_i}\right)\right) = (4.274 \pm 0.094)\text{eV}, \quad (1)$$

with the electron affinity $\chi_{Si} = 4.05$ eV and the band gap $E_g = 1.12$ eV for Si at room temperature, we obtain $\Phi_M = 4.274 \pm 0.094$ eV as the work function of $Mn_5Ge_3C_{0.8}$. For a metal/n-Ge Schottky contact where Fermi level pinning does not play a role, the Schottky barrier height (SBH) is determined by the difference between the metal work function and the electron affinity $\chi_{Ge} = 4.0$ eV of Ge [21]. The efficiency of a spin-injecting metal/semiconductor structure has been shown theoretically to depend strongly on the SBH at the interface, with a large SBH being detrimental to spin injection [22], and the use of a metal with a lower work function than, e.g., Co ($\Phi_{M,\,Co} = 5.0$ eV) or Fe ($\Phi_{M,\,Fe} = 4.5$ eV) could potentially reduce the SBH. Our measurement shows $Mn_5Ge_3C_{0.8}$ to have a work function comparable to that of Fe_3Si ($\Phi_{M,\,Fe3Si} = 4.3$ eV [23]), which was successfully used for spin injection into n-Ge from a Fe_3Si/n-Ge contact [9].

The TLM structures that were used to probe the specific contact resistivity r_C consist of contact pads of width $W = 200$ μm and length $L = 100$ μm spaced $d_i = 3$ to 168 μm apart as shown schematically in figure 3(*a*). *I–V* curves between adjacent contact pads of samples A and B show ohmic behavior with only slight nonlinearities; see figure 3(*b*). The resistance R_{TLM} depends on both the contact resistance R_C of the metal–semiconductor contact and the sheet resistance R_{SH} of the semiconductor according to

$$R_{TLM} = 2R_C + \frac{R_{SH}}{W} \cdot d. \quad (2)$$

For both samples A and B, R_{TLM} is dominated by the contact resistance. The sheet resistance R_{SH} of the n-Ge layer underneath the contacts, estimated to be $R_{SH} = 200$ $\Omega/\square$ in our sample, cannot be extracted from the data due to the scatter of the data points (figure 3(*c*)). Setting $R_{TLM} \approx 2\,R_C$, we obtain an average of $R_C = 26.9$ kΩ for sample A and an average of $R_C = 25.1$ kΩ for sample B. Furthermore, assuming $R_C = r_C/(W \times L)$, we obtain a specific contact resistivity of $r_C = 5.4$ Ω cm^2 for sample A and $r_C = 5.0$ Ω cm^2 for sample B, thus indicating that the substrate temperature in the range investigated here has negligible influence on r_C. The temperature dependence of the specific contact resistivity as obtained from a measurement between adjacent contact pads of sample B is shown in figure 4. A strong dependence of the specific contact resistivity on temperature can be observed.

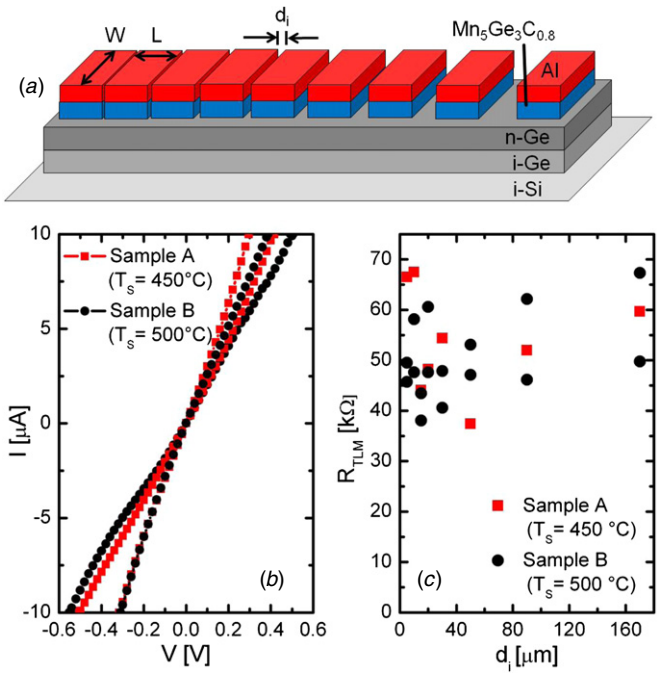

Figure 3. (*a*) Schematic drawing of the transmission-line measurement (TLM) structures. The contact pads each have a width $W = 200$ μm and length $L = 100$ μm and are spaced apart by d_i increasing from 3 to 168 μm. (*b*) *I–V* characteristics obtained from measurements between adjacent contact pads of the TLM structures. Ohmic behavior can clearly be observed for the Al/$Mn_5Ge_3C_{0.8}$ contact on n-Ge ($N_D = 1 \times 10^{20}$ cm^{-3}). (*c*) Resistance R_{TLM} obtained from TLM measurements. R_{TLM} is dominated by the contact resistances, and specific contact resistivities $r_C = 5.4$ Ω cm^2 for sample A and $r_C = 5.0$ Ω cm^2 for sample B can be extracted, indicating a negligible influence of the substrate temperature T_S.

For sample B, we also obtained *I–V* characteristics shown in figure 5(*b*) from three Schottky diodes fabricated on the same sample. By fitting the forward current I_D (V_{DS}) to [21]

$$I_D = A \cdot J_s \cdot \exp\left(\frac{-V_{DS} - R_S \cdot I_D}{\eta \cdot k_B \cdot T/q}\right), \quad (3)$$

where A is the diode area and J_s is the saturation current density, we extract a series resistance $R_S = 60$ kΩ and an ideality factor $\eta = 6.0$. Assuming that the series resistance is dominated by the $Mn_5Ge_3C_{0.8}$/n-Ge contact resistance and given the fact that the size of the Al/$Mn_5Ge_3C_{0.8}$ contact to the n-Ge layer is 1.8×10^{-4} cm^2, we obtain a specific contact resistivity of $r_C \approx 10$ Ω cm^2, which is larger than the specific contact resistivity of the $Mn_5Ge_3C_{0.8}$/n-Ge contact but is consistent

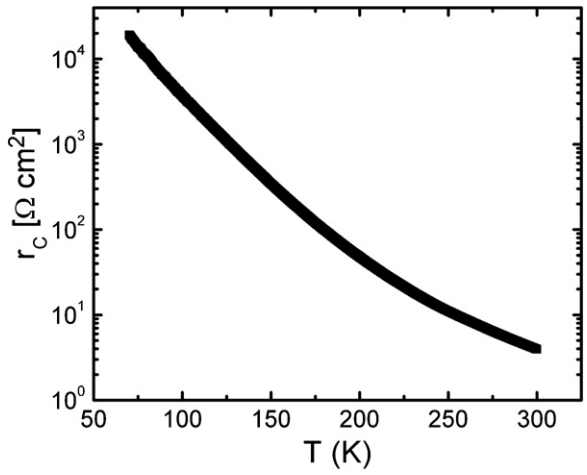

Figure 4. Temperature dependence of the specific contact resistivity as measured between adjacent contact pads of a TLM structure of sample B for temperatures between 70 and 300 K. The specific contact resistivity shows a strong temperature dependence as temperature is decreased.

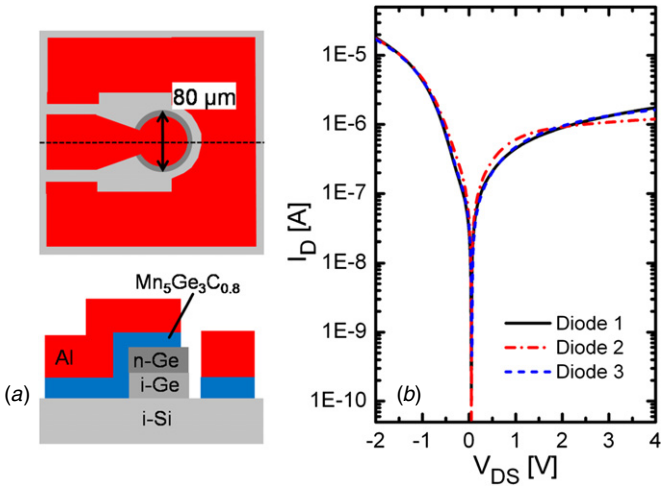

Figure 5. (*a*) Schematic drawing of the fabricated Schottky diodes. $Mn_5Ge_3C_{0.8}$ forms an ohmic contact with the n-Ge ($N_D = 1 \times 10^{20}$ cm^{-3}) and a Schottky contact with the i-Si ($\rho > 40$ Ω cm). (*b*) *I–V* characteristics from three Schottky diodes. Measurements from diodes 1 and 3 are indistinguishable. A series resistance of $R_S = 60$ kΩ can be extracted from the forward characteristics and is consistent with the assumption that the series resistance is dominated by the $Mn_5Ge_3C_{0.8}$/n-Ge contact resistance and the magnitude of the specific contact resistivity obtained from TLM measurements.

in magnitude with the specific contact resistivity extracted from TLM measurements. The high value for η is attributed to defects in the MBE-grown Ge layers.

In general, low-resistive ohmic contacts to n-Ge are difficult to achieve because of strong Fermi-level pinning. The reason for this is currently not fully understood. For Ge, the charge neutrality level, i.e., the position of the Fermi level at which the Ge surface carries no net charge, is positioned just above the valence band, which results in a weak dependence of the SBH on the metal work function and a large SBH of 0.49–0.64 eV for a wide range of metal work functions [24, 25]. Schottky contacts of Mn_5Ge_3 on (lightly doped) Ge (1 0 0) and Ge (1 1 1) have been investigated previously [15, 26] and a SBH of ∼0.6 eV for Mn_5Ge_3 on n-Ge (1 0 0) with a dopant density of $\sim 5 \times 10^{14}$ cm^{-3} was determined [26]. If the n-Ge is highly doped, as is the case for our samples, the width of the Schottky barrier is reduced to a few nanometers and we could expect field emission to be the dominant current transport mechanism. Indeed, our contacts are ohmic, but the specific contact resistivities are large. Furthermore, temperature-dependent measurements of the specific contact resistivity show a strong dependence of the specific contact resistivity on temperature. One possible explanation is interdiffusion of Ge between the $Mn_5Ge_3C_{0.8}$ film and the n-Ge layer, which might lead to the local formation of other phases at the interface that could increase the specific contact resistivity. However, the filling of the interstitial sites of Mn_5Ge_3 by carbon seems to prevent long-range Ge diffusion from the substrate [19]. Another possible cause could be the diffusion of Sb dopants from the substrate into $Mn_5Ge_3C_{0.8}$ during the deposition process, which effectively enlarges the depletion layer in Ge at the interface and, thus, increases the width of the Schottky barrier. A detailed investigation of the Ge/$Mn_5Ge_3C_{0.8}$ interface by transmission electron microscopy and time-of-flight secondary ion mass spectroscopy is necessary to clarify this issue.

4. Conclusion

In this study, we determined the work function $\Phi_M = 4.274 \pm 0.094$ eV of $Mn_5Ge_3C_{0.8}$ from MOS capacitance measurements and measured a specific contact resistivity $r_C = 5.0$ Ω cm^2 at room temperature for $Mn_5Ge_3C_{0.8}$ on highly doped n-Ge. Our investigation serves as a starting point to engineer $Mn_5Ge_3C_x$ contacts for spin injection as a step toward CMOS-compatible spin device fabrication. Future experiments will be directed toward improving the specific contact resistivity of $Mn_5Ge_3C_x$ contacts on n-Ge and investigating the specific contact resistivity of $Mn_5Ge_3C_x$ on highly doped p-Ge, which can be expected to be lower because of a lower SBH. Finally, it will be interesting to investigate the influence of C-doping on the contact resistance and also compare the results with Mn_5Ge_3 contacts obtained by germanidation processes after depositing Mn directly on highly doped n-Ge or p-Ge [27].

References

[1] Datta S and Das B 1990 *Appl. Phys. Lett.* **56** 665
[2] Sugahara S and Tanaka M 2004 *Appl. Phys. Lett.* **84** 2307
[3] Schmidt G, Ferrand D, Molenkamp L W, Filip A T and Van Wees B J 2000 *Phys. Rev.* B **62** R4790
[4] Rashba E I 2000 *Phys. Rev.* B **62** R16267
[5] Appelbaum I, Huang B and Monsma D J 2007 *Nature* **447** 295
[6] Jonker B T, Kioseoglou G, Hanbicki A T, Li C H and Thompson P E 2007 *Nature Phys.* **3** 542
[7] Ando Y, Hamaya K, Kasahara K, Kishi Y, Ueda K, Sawano K, Sadoh T and Miyao M 2009 *Appl. Phys. Lett.* **94** 182105
[8] Zhou Y, Han W, Chang L T, Xiu F, Wang M, Oehme M, Fischer I A, Schulze J, Kawakami R K and Wang K L 2011 *Phys. Rev.* B **84** 125323
[9] Kasahara K, Baba Y, Yamane K, Ando Y, Yamada S, Hoshi Y, Sawano K, Miyao M and Hamaya K 2012 *J. Appl. Phys.* **111** 07C503

[10] Iba S, Saito H, Spiesser A, Watanabe S, Jansen R, Yuasa S and Ando K 2012 *Appl. Phys. Express* **5** 053004
[11] Panguluri R P, Zeng C, Weitering H H, Sullivan J M, Erwin S C and Nadgorny B 2005 *Phys. Status Solidi* b **242** R67
[12] Dedkov Y S, Holder M, Mayer G, Fonin M and Preobrajenski A B 2009 *J. Appl. Phys.* **105** 073909
[13] Zeng C, Erwin S C, Feldman L C, Li A P, Jin R, Song Y, Thompson J R and Weitering H H 2003 *Appl. Phys. Lett.* **83** 5002
[14] Olive-Mendez S, Spiesser A, Michez L A, Le Thanh V, Clachant A, Derrien J, Devilliers T, Barski A and Jamet M 2008 *Thin Solid Films* **517** 191
[15] Sellai A, Mesli A, Petit M, Le Thanh V, Taylor D and Henini M 2012 *Semicond. Sci. Technol.* **27** 035014
[16] Gajdzik M, Sürgers C, Kelemen M and Löhneysen H v 2000 *J. Magn. Magn. Mater.* **221** 248
[17] Sürgers C, Potzger K, Strache T, Möller W, Fischer G, Joshi N and v Löhneysen H 2008 *Appl. Phys. Lett.* **93** 062503
[18] Spiesser A *et al* 2011 *Phys. Rev.* B **84** 165203
[19] Spiesser A, Le Tanh V, Bertaina S and Michez L A 2011 *Appl. Phys. Lett.* **99** 121904
[20] Nicollian E H and Brews J R 2002 *MOS (Metal Oxide Semiconductor) Physics and Technology* (Hoboken, NJ: Wiley)
[21] Sze S M and Ng K K 2006 *Physics of Semiconductor Devices* (Hoboken, NJ: Wiley)
[22] Albrecht J D and Smith D L 2003 *Phys. Rev.* B **68** 035340
[23] Hamaya K, Ando Y, Sadoh T and Miyao M 2011 *Japan. J. Appl. Phys.* **50** 010101
[24] Dimoulas A, Tsipas P, Sotiropoulos A and Evangelou E K 2006 *Appl. Phys. Lett.* **89** 252110
[25] Nishimura T, Kita K and Toriumi A 2007 *Appl. Phys. Lett.* **91** 123123
[26] Nishimura T, Nakatsuka O, Akimoto S, Takeuchi W and Zaima S 2011 *Microelectron. Eng.* **88** 605
[27] Tang J *et al* 2012 *ACS Nano* **6** 5710